



Ultra-high b value DWI in distinguishing fresh gray matter ischemic lesions from white matter ones: a comparative study with routine and high b value DWI

Xinming Huang^{1#}, Xue Xu^{1#}, Yifan Sun¹, Guoen Cai², Rifeng Jiang^{1^}, Jianhua Chen¹, Yunjing Xue¹

¹Department of Radiology, Fujian Medical University Union Hospital, Fuzhou, China; ²Department of Neurology, Fujian Medical University Union Hospital, Fuzhou, China

Contributions: (I) Conception and design: R Jiang, G Cai; (II) Administrative support: Y Xue, J Chen; (III) Provision of study materials or patients: G Cai; (IV) Collection and assembly of data: X Huang, X Xu, Y Sun; (V) Data analysis and interpretation: R Jiang, X Huang, Y Sun; (VI) Manuscript writing: All authors; (VII) Final approval of manuscript: All authors.

[#]These authors contributed equally to this work.

Correspondence to: Rifeng Jiang, PhD. Department of Radiology, Fujian Medical University Union Hospital, No. 29 Xinquan Road, Fuzhou 350001, China. Email: 26630706@qq.com; Guoen Cai, PhD. Department of Neurology, Fujian Medical University Union Hospital, No. 29 Xinquan Road, Fuzhou 350001, China. Email: 36991045@qq.com.

Background: Fresh ischemic lesions (FILs) can occur in both the brain's gray matter (GM) and white matter (WM), with each location signifying a different prognosis for patients. This study aims to investigate the application of ultra-high b value diffusion-weighted imaging (DWI) in distinguishing FILs in these two areas via a comparative study with routine and high b value DWI.

Methods: Multiple b value DWI (b=0, 500, 1,000, 2,000, 4,000, 6,000, 8,000, 10,000 s/mm²) was performed on 47 patients with suspected acute ischemic stroke (AIS). Apparent diffusion coefficient (ADC) maps, including ADC₅₀₀, ADC_{1,000}, ADC_{2,000}, ADC_{4,000}, ADC_{6,000}, ADC_{8,000}, and ADC_{10,000}, were calculated, and the mean ADC value of the FILs in the GM and WM on each map was obtained by referring to the structural magnetic resonance imaging (MRI). ADC value differences of the FILs in the GM and WM were compared using Mann-Whitney U tests, and receiver operating characteristic (ROC) curves evaluated the diagnostic efficiency of each ADC value in distinguishing FILs in the two areas.

Results: In the enrolled 34 patients, 145 FILs were identified, of which 42 involved the GM, 87 the WM, and 16 both the GM and WM. A total of 161 regions were delineated, 58 in the GM and 103 in the WM. The values of FILs in the WM on ADC_{2,000}, ADC_{4,000}, ADC_{6,000}, ADC_{8,000}, and ADC_{10,000} maps were significantly lower than those in the GM (P=0.007, P<0.001, P<0.001, P<0.001 and P<0.001, respectively), while no significant differences were found on ADC₅₀₀ and ADC_{1,000} maps (P=0.427 and P=0.225, respectively). ROC curves demonstrated that the area under the curve (AUC) paralleled the increasing b value, ascending from ADC₅₀₀ to ADC_{10,000} (0.538, 0.558, 0.629, 0.766, 0.827, 0.859, 0.872, in that order).

Conclusions: Ultra-high b value DWI is extremely sensitive to the slight diffusion difference between FILs in the GM and the WM. Its sensitivity parallels the increasing b value, indicating its clinical advantage in identifying the microstructure of FILs.

Keywords: Ultra-high b value diffusion-weighted imaging (ultra-high b value DWI); acute ischemic stroke (AIS); fresh ischemic lesion (FIL); gray matter (GM); white matter (WM)

[^] ORCID: 0000-0001-6959-0027.

Submitted Nov 05, 2020. Accepted for publication May 28, 2021.

doi: 10.21037/qims-20-1241

View this article at: <https://dx.doi.org/10.21037/qims-20-1241>

Introduction

As a significant cause of human mortality and disability, stroke is often induced by ischemia, with ischemic stroke imposing substantial social and economic burden worldwide (1,2).

Of the diagnostic means to assess acute ischemic stroke (AIS), diffusion magnetic resonance imaging (dMRI), accompanied by diffusion models such as the mono-exponential model, bi-exponential model, diffusion kurtosis model, and neurite orientation dispersion and density imaging, is widely used to evaluate acute cerebral ischemic lesions (3-8). In clinical practice, diffusion-weighted imaging (DWI) is the most frequently used diffusion technique, which can noninvasively reflect the diffusion of water molecules in tissues by providing an apparent diffusion coefficient (ADC) map. The latter is typically calculated with the mono-exponential model, which usually needs two b value (0 and 1,000 s/mm²) images of the brain (9). Recently, high b value and ultra-high b value DWI are more frequently applied due to the popularity of 3.0- and even 7.0-Tesla MR systems (6,7,10-12). With the increased intensity of the diffusion gradient, such as 80 mT/m and 200 T/m/s used in the MAGNETOM Prisma, the application of the diffusion gradient can be completed within a much shorter timeframe, thereby greatly reducing the echo time (TE) and increasing the signal-to-noise ratio, as shown in [Figure S1](#). At present, the b value of DWI can be as high as 10,000 s/mm², making it more powerful in differentiating the diffusion subtleties of water molecules in different tissues (13-15).

Fresh ischemic lesion (FIL) can occur in both the gray matter (GM) and the white matter (WM) of the brain, and each location may signify varied severity of the clinical manifestations as well as a different prognosis for patients (16,17). It is important to accurately identify the location in GM or WM for FIL because GM and WM in the brain have considerably different perfusion properties and neurochemical responses to ischemia (18,19). In patients who survived a brief period of cardiac arrest, laminar necrosis in the cerebral cortex and severe ischemic changes in the basal ganglia were present, while there were only minor changes in the WM (20). Additionally,

recent research suggests that thresholds in AIS diagnosis should be varied for acute infarction in both the GM and the WM to provide a more accurate estimation of acute ischemic core (21). Other research has found that GM has a higher infarction threshold for cerebral blood flow (CBF), cerebral blood volume (CBV), and ADC than WM in patients within 24 hours of ischemic stroke onset (22). Therefore, accurate identification of FIL in the GM or WM may have potential clinical significance for treatments and prognosis of AIS patients. However, on structural MRI and conventional DWI scans, the difference in intensity between FILs in GM and WM is not always obvious. In these cases, it becomes difficult to determine the location of lesions, thus greatly reducing the diagnostic accuracy for GM and WM location.

Previous studies have reported that with the increase of b value, the mean DWI intensity over a region of interest (ROI) declines much more slowly in WM than in GM, indicating that the diffusion of water molecules is much more restricted in WM than in GM (23). Another study found that the mean ADC value was significantly greater in GM than that in WM (24). In other words, there is an inherent contrast in DWI intensity between normal GM and WM. Additionally, the ADC_{1,000} value was also greater in GM proportions of acute ischemic cores than that in WM proportions, although not reaching significance (22). Therefore, in diagnosing FILs in the GM and WM, we speculate that the diffusion difference in water molecules of FILs in these two regions may also induce distinct signal intensity in a scenario involving ultra-high b value DWI. To date, however, few studies focus on the differentiation of FILs in the GM and WM, let alone the application of the ultra-high b value DWI to the distinction.

It is generally accepted that different b values of DWI have a varied potential for disease diagnosis (5-7,12,25). Therefore, it is important to compare the diagnostic efficacy and reliability of different ADC values to design optimal scan protocols. In the current study, multiple b value DWI, including routine, high and ultra-high b values, was employed to evaluate the role of ultra-high b value DWI in distinguishing FILs in the GM and the WM and its diagnostic efficiency compared to routine and high b value DWI.

Methods

Inclusion and exclusion criteria for patients

The study was conducted following the Declaration of Helsinki (as revised in 2013). The ethics committee board approved the study of Fujian Medical University Union Hospital, and informed consent was taken from all the patients. Enrolled patients and FILs were subject to the following inclusion criteria: (I) a group of random patients suspected of having FILs within the acute (0 hour–3 days) or subacute (3 days–2 weeks) stage, based on the time from symptom onset to MRI examination; (II) the patients underwent structural MRI and 8 b value DWI of the brain with the same scanner; (III) the lesions were FILs, which were defined as ischemic lesions with high intensity on DWI of all b values; (IV) the FIL was categorically located in the GM or the WM, and for lesions involving both the GM and WM, a part of the GM or WM portion should be clearly identified. The exclusion criteria were as follows: (I) patients without any FILs or with FILs solely in the cerebellum or brainstem; (II) patients with motion artifacts or poor image quality; (III) FILs located in the cerebellum, pons, and medulla were excluded if a patient contained FILs in both the cerebrum and cerebellum or brainstem.

Between May 2018 and June 2019, in a random series, 47 patients with suspected AIS underwent structural MRI and 8 b value DWI of the brain. Among them, 10 patients were excluded due to the absence of FILs (n=6) or the presence of FILs solely in the cerebellum or brainstem (n=4), and 3 patients were excluded due to poor image quality or motion artifact. Thirty-four patients (19 males and 15 females; mean age: 67.06±12.61 years within the range of 35–88 years) were enrolled in the current study, with 8 patients in the acute stage (38.50±13.93 hours) and 26 in the subacute stage (142.15±72.42 hours). The National Institutes of Health stroke scale (NIHSS) admission score for these patients was 5.03±4.32. Signs and symptoms of the enrolled patients included weakness of the body on one side, problems in speaking, dizziness, and loss of vision.

Brain MR imaging

MRI examinations of the whole brain were conducted on a 3.0-T MRI system (MAGNETOM Prisma, Siemens Healthcare, Erlangen, Germany) with a 64-channel receive-only head coil. The structural MRI and multi-b-value DWI were performed during the same examination.

The structural MRI sequences were: T2-weighted fast

spin echo in the transverse planes [repetition time (TR)/TE, 6,000 ms/99 ms; acquisition matrix, 320×320; field of view (FOV), 23 cm × 23 cm; number of excitation (NEX), 1; slice thickness, 5 mm; gap, 1 mm]; fluid-attenuated inversion recovery (FLAIR) in the transverse plane (TR/TE, 9,000 ms/81 ms; inversion time, 2,500 ms; acquisition matrix, 320×224; FOV, 23 cm × 23 cm; NEX, 1; slice thickness, 5 mm; gap, 1 mm); and sagittal T1-MPRAGE (TR/TE, 2,300 ms/2.32 ms; inversion time, 900 ms; acquisition matrix, 256×256; FOV, 24 cm × 24 cm; NEX, 1; acquisition voxel size: 0.9375×0.9375×0.9 mm³). Sagittal T1-MPRAGE images were also registered to the b0 image using the Image Registration tool in DiffusionKit and subsequently reconstructed as transverse images used as structural references for ROI delineation.

A single-shot echo planer imaging sequence was used for the multi-b-value DWI imaging with the following parameters: TR/TE, 3,800 ms/74 ms; slice thickness, 5 mm, gap, 1 mm; FOV, 23 cm × 23 cm; phase FOV, 1.00; acquisition matrix, 128×128, reconstruction matrix, 256×256; GRAPPA, 2; slice acceleration factor, 2; and pixel bandwidth, 2055 Hz/pixel. The sequence was performed with 8 b values (0, 500, 1,000, 2,000, 4,000, 6,000, 8,000 and 10,000 s/mm²) in a 4-Scan-Trace mode, which uses four diffusion gradient directions for each b value. The number of scan averages for b=0 to 10,000 s/mm² were 1, 1, 1, 2, 3, 3, 4 and 6, respectively. The total scan time was 5 min 28 s.

MR DWI analysis

All diffusion-weighted images underwent motion correction by co-registering DWI images to b0 images with the DiffusionKit (<https://diffusionkit.readthedocs.io/en/latest/#>). ADC maps of b values ADC₅₀₀, ADC_{1,000}, ADC_{2,000}, ADC_{4,000}, ADC_{6,000}, ADC_{8,000} and ADC_{10,000} were calculated by fitting the b0 image and DWI images of other b values into the mono-exponential equation: $S_b/S_0 = \exp(-b \times \text{ADC})$ (11), where S_b is the diffusion-weighted signal intensity for the b value, and S_0 is the signal intensity obtained with b=0.

Quantitative image analysis

For accurately delineating and determining the location of the FILs, a strict screening process was adopted. In brief, two radiologists (Dr. RJ and YS, with 8 and 5 years of experience, respectively) evaluated all FILs independently using ImageJ software (Version 1.49o, National Institutes

of Health). The structural MRI images were carefully reviewed to determine the location of the FILs. For FILs involving GM or WM, the ROI was delineated over the whole lesion on each DWI map. For FILs involving both the GM and WM, a part of the GM or WM portion should be clearly identified, and ROIs for the GM or WM portion were delineated separately. The FILs evaluated by the two radiologists were compared.

Further discussion was arranged for any inconsistent FIL assessments. If a consensus was reached after discussion and the inclusion criteria were met, the FILs were included in the subsequent analysis; otherwise, the FILs were excluded. ROIs over included FILs were further used to calculate the mean ADC values, including ADC_{500} , $ADC_{1,000}$, $ADC_{2,000}$, $ADC_{4,000}$, $ADC_{6,000}$, $ADC_{8,000}$, and $ADC_{10,000}$. The final location results for ROIs after discussion served as a reference standard to assess diagnostic accuracy.

Statistical analysis

Statistical analyses were performed with IBM SPSS 20.0 software (IBM Corp, Chicago, IL, USA) and MedCalc 11.4.2.0 (<http://www.medcalc.be/>). The intraclass correlation coefficient (ICC) was also used to assess the data consistency of repeated measures of the same parameter. ICC values <0.50 were considered poor, 0.50–0.75 moderate, 0.75–0.90 good, and >0.90 excellent (11). Bland-Altman plots were created to investigate systematic bias. Mann-Whitney U tests were performed to compare the differences in ADC_{500} , $ADC_{1,000}$, $ADC_{2,000}$, $ADC_{4,000}$, $ADC_{6,000}$, $ADC_{8,000}$, and $ADC_{10,000}$ values between FILs in the GM and the WM because most of the ADC values did not pass Tests of Normality. Receiver operating characteristic (ROC) analyses were further performed to determine the diagnostic efficiency of each ADC value, the optimal thresholds, diagnostic sensitivity, and specificity for differentiating the FILs in the GM and the WM. The Z test was adopted to compare the area under the curves (AUCs) of the ADC maps. $P < 0.05$ indicated a statistically significant difference.

Results

FILs

The two radiologists found 183 measurable FILs in the 34 patients, with 123 consistent lesions and 60 inconsistent ones. After discussion, 22 lesions were excluded due to

undetermined GM or WM location, and another 16 were excluded for being located in the cerebellum, pons, or medulla. The screening process and measurement of the FILs by the two radiologists are described in detail in available online: <https://cdn.amegroups.cn/static/public/qims-20-1241-1.pdf>. Of the 145 FILs, 42 lesions involved the GM, 87 the WM, and 16 GM and WM. A total of 161 ROIs were delineated, including 58 ROIs in the GM or GM nuclei ($113.30 \pm 223.24 \text{ cm}^2$ in the area for Dr. RJ and $77.04 \pm 101.68 \text{ cm}^2$ for Dr. YS) and 103 in the WM ($72.56 \pm 124.12 \text{ cm}^2$ in the area for Dr. RJ and $63.32 \pm 102.46 \text{ cm}^2$ for Dr. YS), as shown in *Figure 1*.

Inter-observer consistency in measure

The consistency of repeated measures of the two radiologists was first evaluated. The ICC for inter-observer consistency was 0.953–0.975 for the ROIs in the GM and 0.951–0.973 for those in the WM, indicating excellent inter-observer reproducibility (*Table 1*). The Bland Altman plot showed no obvious systematic bias between the measures of the two radiologists (*Figure 2*). Due to Dr. RJ's seniority and rich clinical experiences, the measurement data from Dr. RJ were further used for subsequent statistical analysis.

ADC differences between FILs in the WM and the GM

The median values and interquartile ranges of the ADC values of FILs in the GM and the WM are summarized in *Table 2*. Mann-Whitney U tests demonstrated that the $ADC_{2,000}$, $ADC_{4,000}$, $ADC_{6,000}$, $ADC_{8,000}$, and $ADC_{10,000}$ values of FILs in the WM were significantly lower than those in the GM ($P = 0.007$ for $ADC_{2,000}$ and $P < 0.001$ for the rest); in contrast, no significant differences between the two areas were found in the ADC_{500} and $ADC_{1,000}$ values ($P = 0.427$ and $P = 0.225$, respectively) of FILs.

Comparison of diagnostic efficiency of different ADC values

ROC curves were then constructed (*Figure 3*). The AUCs of ADC_{500} , $ADC_{1,000}$, $ADC_{2,000}$, $ADC_{4,000}$, $ADC_{6,000}$, $ADC_{8,000}$ and $ADC_{10,000}$ were 0.538, 0.558, 0.629, 0.766, 0.827, 0.859 and 0.872, respectively, indicating that the diagnostic efficiency of ADC improved with the increasing b value. The optimal thresholds, sensitivity, and specificity of each ADC value for differentiating FILs in the two areas are shown in *Table 3*. Of all the ADC values, $ADC_{10,000}$ achieved

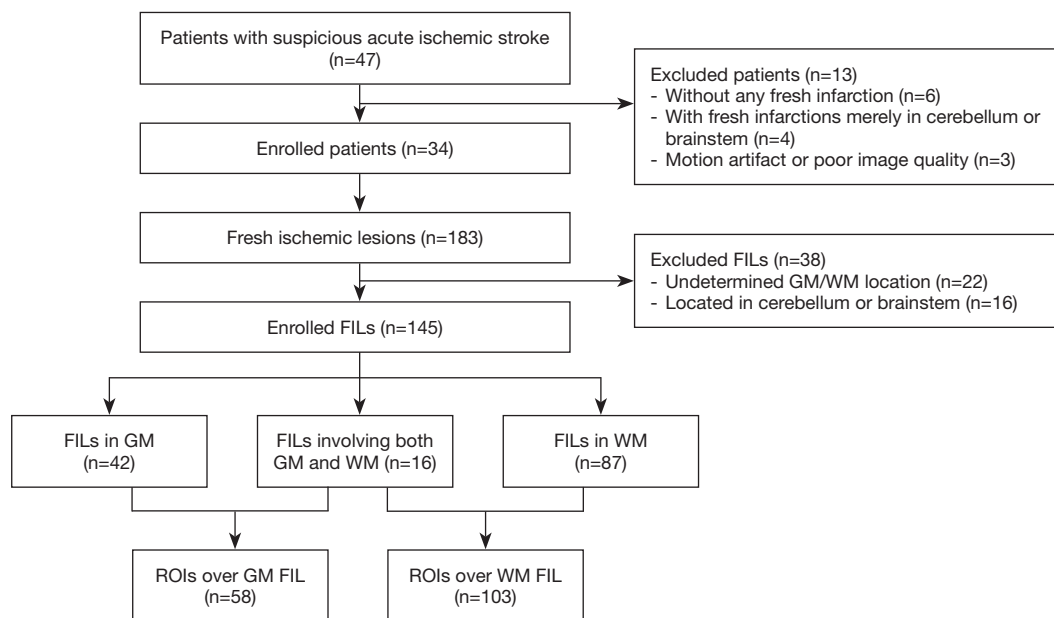


Figure 1 Screening process for the enrolled patients and FILs. FIL, fresh ischemic lesion; GM, gray matter; WM, white matter; ROI, region of interest.

Table 1 Inter-observer reproducibility in measurement of FILs

Region	Metrics	ICC, 95% CI for inter-observer
FILs in GM (n=58)	ADC ₅₀₀	0.953, 0.922–0.972
	ADC _{1,000}	0.973, 0.954–0.984
	ADC _{2,000}	0.975, 0.958–0.985
	ADC _{4,000}	0.974, 0.956–0.984
	ADC _{6,000}	0.969, 0.949–0.982
	ADC _{8,000}	0.965, 0.942–0.979
	ADC _{10,000}	0.959, 0.932–0.976
FILs in WM (n=103)	ADC ₅₀₀	0.972, 0.959–0.981
	ADC _{1,000}	0.967, 0.952–0.978
	ADC _{2,000}	0.972, 0.958–0.981
	ADC _{4,000}	0.973, 0.961–0.982
	ADC _{6,000}	0.964, 0.947–0.975
	ADC _{8,000}	0.959, 0.941–0.972
	ADC _{10,000}	0.951, 0.928–0.966

FIL, fresh ischemic lesion; ICC, intraclass correlation coefficient; CI, confidence interval; ADC, apparent diffusion coefficient; GM, gray matter; WM, white matter.

the highest diagnostic efficiency, with a sensitivity of 86.21%, a specificity of 77.67%, and an AUC of 0.872 at a cut-off value of $2.048 \times 10^{-4} \text{ mm}^2/\text{s}$. The AUC of ADC_{10,000} was significantly higher than those of ADC of routine b values (ADC₅₀₀: Z=8.147, P<0.001 and ADC_{1,000}: Z=7.781, P<0.001), high-b values (ADC_{2,000}: Z=7.347, P<0.001 and ADC_{4,000}: Z=5.529, P<0.001), and even the other two ultra-high b values (ADC_{6,000}: Z=4.424, P<0.001 and ADC_{8,000}: Z=2.735, P=0.006). Two examples demonstrating the ADC difference between FILs in the GM and that in the WM by ultra-high-b-value DWI are shown in *Figure 4*.

Discussion

The current study found that ADC_{2,000}, ADC_{4,000}, ADC_{6,000}, ADC_{8,000}, and ADC_{10,000} values of FILs in the WM were significantly lower than those in the GM without significant differences between these two areas in ADC₅₀₀ and ADC_{1,000} values were evident. Of interest, the study found that compared with high b value DWI, ultra-high b value DWI had a higher precision in delineating the diffusion difference of water molecules in the fresh GM and WM ischemia, signifying its potential clinical value

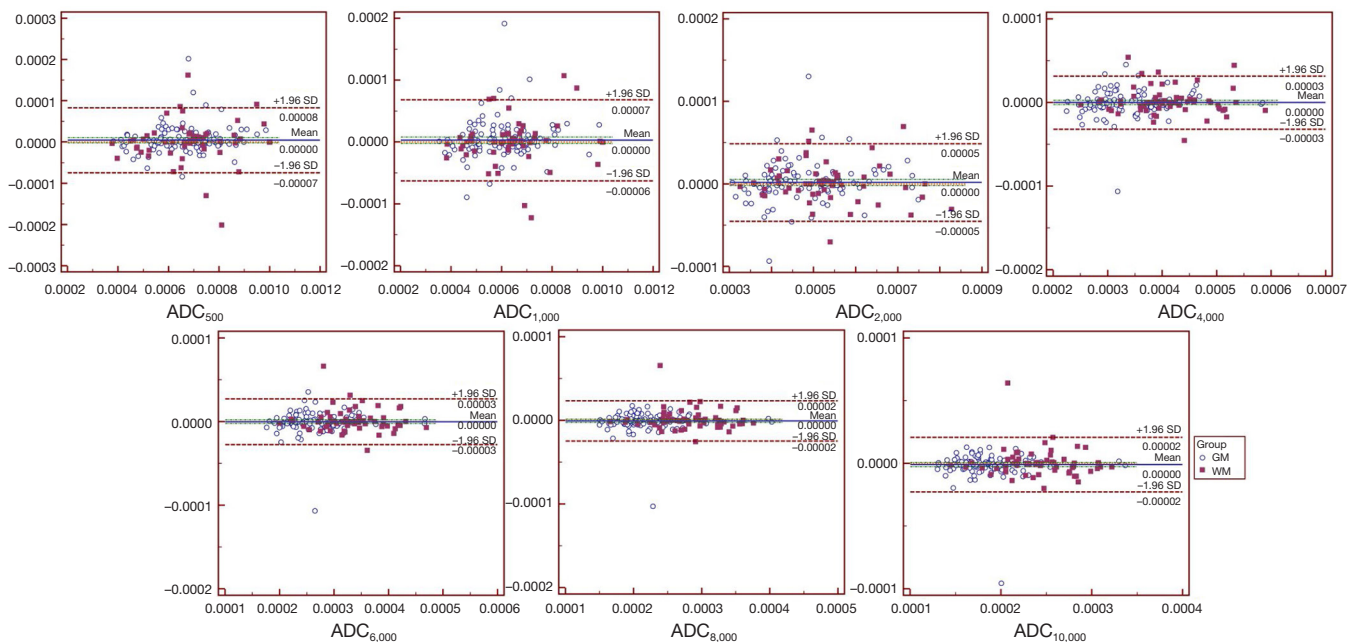


Figure 2 Bland-Altman plots for inter-observer reliability of all ADC values. The center solid lines represent MD. Upper and lower dotted lines represent the LOA, defined as the MD \pm 1.96 \times SD of the difference in measurement between the two radiologists. The unit of ADC is mm²/s. ADC, apparent diffusion coefficient; MD, mean difference; LOA, limit of agreement; SD, standard deviation; GM, gray matter; WM, white matter.

Table 2 ADC differences between FILs in WM and GM

ADC value	FILs in GM (n=58)	FILs in WM (n=103)	Z	P value
ADC ₅₀₀	6.981 (5.930–7.709)	6.762 (5.732–7.832)	-0.794	0.427
ADC _{1,000}	6.339 (5.593–6.967)	6.120 (5.065–6.962)	-1.213	0.225
ADC _{2,000}	5.244 (4.741–5.671)	4.676 (3.990–5.537)	-2.708	0.007*
ADC _{4,000}	4.082 (3.657–4.590)	3.277 (2.890–3.810)	-5.595	<0.001*
ADC _{6,000}	3.312 (2.995–3.745)	2.583 (2.284–2.967)	-6.872	<0.001*
ADC _{8,000}	2.783 (2.524–3.211)	2.124 (1.896–2.413)	-7.551	<0.001*
ADC _{10,000}	2.397 (2.169–2.732)	1.817 (1.647–2.025)	-7.826	<0.001*

* indicates P<0.05. The unit of ADC is 10⁻⁴ mm²/s. ADC, apparent diffusion coefficient; FIL, fresh ischemic lesion; GM, gray matter; WM, white matter.

in identifying the location of ischemic lesions. The use of high b value DWI, particularly ultra-high b value DWI, helps to identify the GM and WM location of FILs as an important finding as well-documented differences in the neurochemical response to ischemia of the WM compared to GM compartments of the brain (18,19). In addition, the differing cellular constituents in GM and WM are associated with differing levels of CBF and metabolism (26);

hence, it would seem likely that each compartment might have a differing vulnerability to ischemia. Indeed, it has been shown in patients who survived a brief period of cardiac arrest that laminar necrosis in the cerebral cortex and severe ischemic changes in the basal ganglia were present, while there were only minor changes in the WM (20). Therefore, ischemic lesions located in the GM may have a different prognosis than those in WM, and consequently, FILs in the

GM and WM should be treated separately.

A recent study found that spatial features of ischemic lesions provide useful information that should be integrated to improve lesion outcome prediction using machine learning models (27). Another study compared the difference in the diffusion kurtosis imaging (DKI)

parameter values of acute ischemic lesions in different locations, some in the GM and some in the WM, including the periventricular WM, corpus callosum, cerebellum, basal ganglia and thalamus, brainstem and gray-white matter junctions (16). The authors reported significant differences in the mean kurtosis among most of the locations, indicating that DKI can identify the heterogeneity difference of lesions in the GM and WM. In contrast, no significant difference was found between most locations in ADC, mean diffusivity, axial diffusivity, or radial diffusivity. In this study, we differentiated FILs in the GM and WM anatomically, with those located in the GM nucleus also incorporated into the GM group. This anatomic classification better reveals the reality of AIS. As expected, we found subtle differences in the diffusion of water molecules in fresh GM and WM ischemic lesions. The greater residual DWI signal intensity of FILs in WM may be first attributed to the inherent contrast between GM and WM. As previously reported (23), with the increase of b values, the mean DWI signal intensity over an ROI declined much more slowly in WM than in GM, indicating that the diffusion of water molecules in WM is much more restricted than in GM. This phenomenon is due to the absence of transmembrane of water molecules across myelin sheaths. In addition, cortex ischemia usually induces swelling of the cortex due to the accumulation of water, which may alleviate the restricted diffusion of the water molecules, resulting in a relatively high ADC compared with FILs in WM. This slight difference in restricted water diffusion may have a potential impact on the functional recovery of AIS patients.

We further found that parallel with the increasing b value, the ability of the corresponding ADC value to identify FILs in the GM and WM gradually improved.

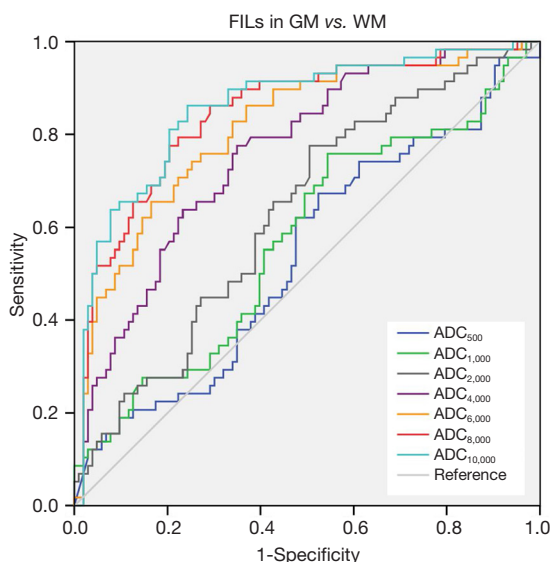


Figure 3 ROC curves of different ADC values in distinguishing FILs in the GM and WM. The AUCs of ADC_{10,000}, ADC_{8,000}, ADC_{6,000}, ADC_{4,000}, ADC_{2,000}, ADC_{1,000} and ADC₅₀₀ were 0.872, 0.859, 0.827, 0.766, 0.629, 0.558 and 0.538, respectively, indicating that the diagnostic efficiency of ADC declined with the decreasing b value. ROC, receiver operating characteristic; ADC, apparent diffusion coefficient; FIL, fresh ischemic lesion; GM, gray matter; WM, white matter; AUC, area under the curve.

Table 3 Diagnostic efficiency of different ADC values in discriminating FILs in WM and GM

ADC	Cut-off value	AUC	Sensitivity	Specificity
ADC ₅₀₀	6.581	0.538	67.2%	47.6%
ADC _{1,000}	6.192	0.558	60.3%	55.3%
ADC _{2,000}	4.742	0.629	75.9%	51.5%
ADC _{4,000}	3.769	0.766	70.7%	72.8%
ADC _{6,000}	2.927	0.827	81.0%	73.8%
ADC _{8,000}	2.439	0.859	84.5%	80.6%
ADC _{10,000}	2.048	0.872	86.2%	77.7%

The 'cut-off value' indicates the optimal threshold in the current study or sample size. The unit of ADC is 10⁻⁴ mm²/s. ADC, apparent diffusion coefficient; FIL, fresh ischemic lesion; GM, gray matter; WM, white matter; AUC, area under the curve.

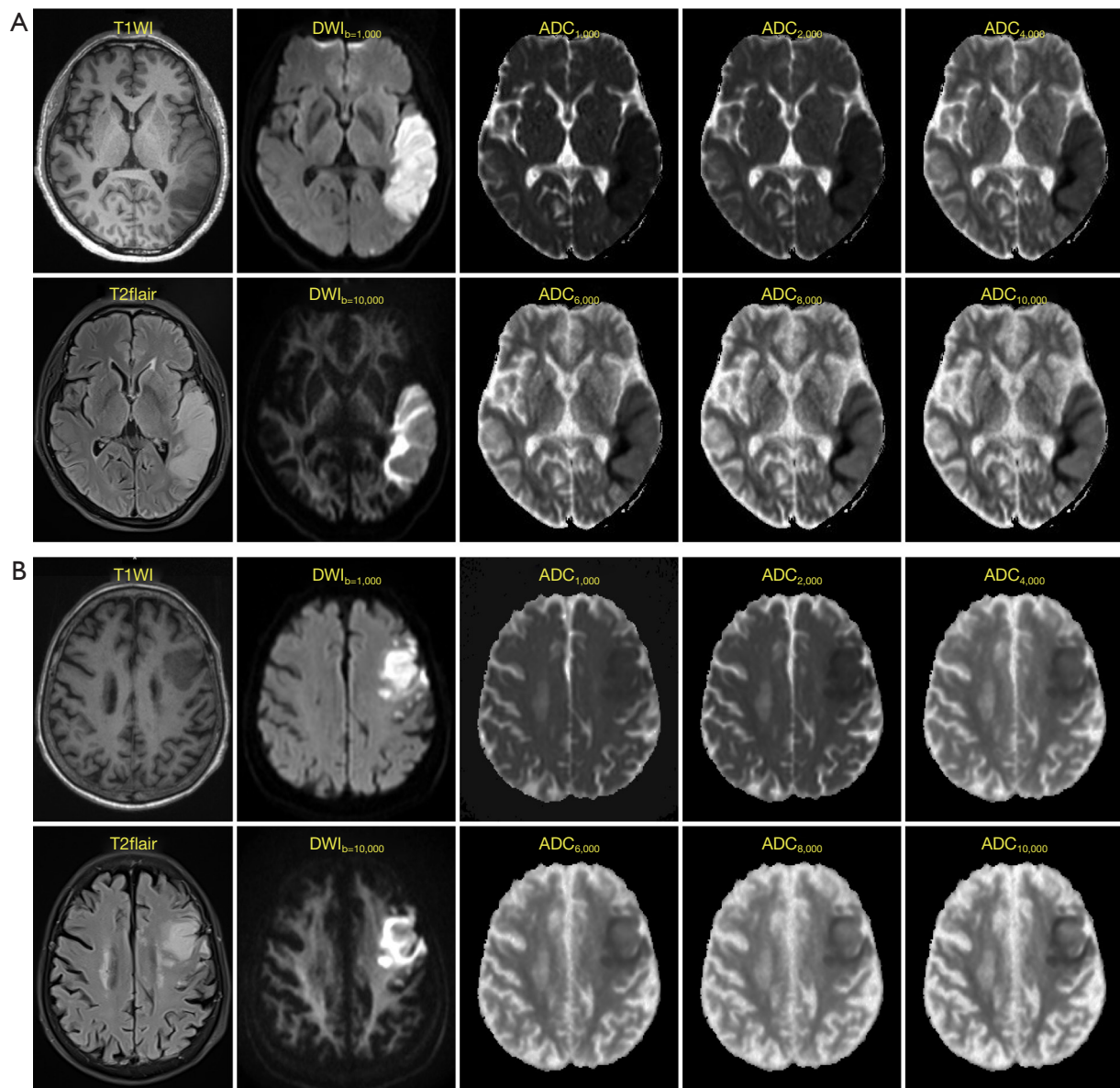


Figure 4 Two representative patients demonstrating the ADC difference between FILs in the GM and that in the WM. Structural MRI (T1WI and T2flair), multiple-b-value DWI and ADC images of a 63-year-old male patient (patient A) and an 83-year-old male patient (patient B) show FILs involving both the GM and the WM were detected in the left temporal lobe and left frontal lobe, respectively. Ultra-high b value DWI ($b=10,000$ s/mm²) clearly distinguished the FIL in the swelling GM portion (the region of lower intensity) and the WM portion (the region of higher intensity), and the ADC difference of these two FIL regions increased as the b value was elevated. ADC, apparent diffusion coefficient; FIL, fresh ischemic lesion; GM, gray matter; WM, white matter; MRI, magnetic resonance imaging; DWI, diffusion-weighted imaging; T1WI, T1-weighted imaging.

When the b value rose to 10,000 s/mm², an optimal differential diagnosis performance was achieved, with an AUC of 0.872. The sensitivity (86.21%) and specificity (77.67%) were optimized when the cut-off value was set as 2.048×10⁻⁴ mm²/s. As the b value rises, the T2 weighted intensity gradually decreases, while the diffusion-weighted intensity and the ability of DWI to identify the diffusion difference also increase. Therefore, with ultra-high b values, DWI can effectively distinguish the very subtle differences in water diffusion so that FILs in the GM and WM can be clearly identified. In contrast, although the intensity of FILs in the GM is different from that in the WM on high b value DWI, the intensity difference of the two lesions is obscure and cannot be easily observed by the naked eye. Therefore, ultra-high b value DWI is superior in differentiating FILs in the GM and WM, providing potential clinical value in symptom determination and prognosis prediction.

This study contains several limitations. Firstly, the number of patients and FILs enrolled in the study was limited, with relatively few FILs involving the GM. Secondly, ischemic lesions in the GM or WM are likely to signify different prognoses for AIS patients; however, longitudinal MRI data, only found for 14.71% (5/34) of patients in this study, were insufficient for making comparisons. Additionally, most of the post-treatment functional performance data such as motor recovery, memory, or higher cognition were not available to confirm the relation between GM/WM location and prognoses. However, the two representative patients shown in Figure S2 seem to demonstrate that FILs in WM may have a better prognosis than those in GM nuclei. Finally, although we adopted a strict screening and discussion process to make the subjective data reliable, the subjective determination of the GM/WM locations for FILs was another limitation. Therefore, the potential clinical significance of identifying fresh GM or WM ischemia still requires further research efforts.

Conclusions

Ultra-high b value DWI is highly sensitive to the subtle diffusion difference present in FILs in the GM and those in the WM, with its sensitivity paralleling the increasing b value, indicating its clinical superiority in identifying the microstructure of FILs.

Acknowledgments

Funding: This work was supported by grants from Joint

Funds for the Innovation of Science and Technology, Fujian province (grant number: 2019Y9074), Outstanding Young Scientific Research Talents Program of Fujian Province (grant number: 2018B050), Youth Foundation of Fujian Provincial Health and Health Commission (grant number: 2014-2-16) and Startup Fund for Scientific Research, Fujian Medical University (grant number: 2017XQ1040 and 2018QH1041).

Footnote

Conflicts of Interest: All authors have completed the ICMJE Uniform Disclosure Form (available at <https://dx.doi.org/10.21037/qims-20-1241>). The authors have no conflicts of interest to declare.

Ethical Statement: The authors are accountable for all aspects of the work in ensuring that questions related to the accuracy or integrity of any part of the work are appropriately investigated and resolved. The study was conducted in accordance with the Declaration of Helsinki (as revised in 2013). The study was approved by the ethics committee board of Fujian Medical University Union Hospital, and informed consent was taken from all the patients.

Open Access Statement: This is an Open Access article distributed in accordance with the Creative Commons Attribution-NonCommercial-NoDerivs 4.0 International License (CC BY-NC-ND 4.0), which permits the non-commercial replication and distribution of the article with the strict proviso that no changes or edits are made and the original work is properly cited (including links to both the formal publication through the relevant DOI and the license). See: <https://creativecommons.org/licenses/by-nc-nd/4.0/>.

References

1. Mozaffarian D, Benjamin EJ, Go AS, Arnett DK, Blaha MJ, Cushman M, et al. Heart disease and stroke statistics-2016 update: a report from the American Heart Association. *Circulation* 2016;133:e38-360.
2. Khatri R, Vellipuram AR, Maud A, Cruz-Flores S, Rodriguez GJ. Current endovascular approach to the management of acute ischemic stroke. *Curr Cardiol Rep* 2018;20:46.
3. Hui ES, Fieremans E, Jensen JH, Tabesh A, Feng W, Bonilha L, Spampinato MV, Adams R, Helpert JA. Stroke

- assessment with diffusional kurtosis imaging. *Stroke* 2012;43:2968-73.
4. Yoo AJ, Gonzalez RG. Clinical applications of diffusion MR imaging for acute ischemic stroke. *Neuroimaging Clin N Am* 2011;21:51-69, vii.
 5. Yin J, Sun H, Wang Z, Ni H, Shen W, Sun PZ. Diffusion kurtosis imaging of acute infarction: comparison with routine diffusion and follow-up MR imaging. *Radiology* 2018;287:651-7.
 6. Lettau M, Laible M. 3-T high-b-value diffusion-weighted MR imaging in hyperacute ischemic stroke. *J Neuroradiol* 2013;40:149-57.
 7. Toyoda K, Kitai S, Ida M, Suga S, Aoyagi Y, Fukuda K. Usefulness of high-b-value diffusion-weighted imaging in acute cerebral infarction. *Eur Radiol* 2007;17:1212-20.
 8. Wang Z, Zhang S, Liu C, Yao Y, Shi J, Zhang J, Qin Y, Zhu W. A study of neurite orientation dispersion and density imaging in ischemic stroke. *Magn Reson Imaging* 2019;57:28-33.
 9. Iima M, Le Bihan D. Clinical intravoxel incoherent motion and diffusion MR imaging: past, present, and future. *Radiology* 2016;278:13-32.
 10. Xueying L, Zhongping Z, Zhousheng Z, Li G, Yongjin T, Changzheng S, Zhifeng Z, Peihao C, Hao X, Li H. Investigation of apparent diffusion coefficient from ultra-high b values in Parkinson's disease. *Eur Radiol* 2015;25:2593-600.
 11. Hu YC, Yan LF, Sun Q, Liu ZC, Wang SM, Han Y, Tian Q, Sun YZ, Zheng DD, Wang W, Cui GB. Comparison between ultra-high and conventional mono b value DWI for preoperative glioma grading. *Oncotarget* 2017;8:37884-95.
 12. Tsubouchi Y, Itamura S, Saito Y, Yamashita E, Shinohara Y, Okazaki T, Ohno K, Nishimura Y, Oguri M, Maegaki Y. Use of high b value diffusion-weighted magnetic resonance imaging in acute encephalopathy/encephalitis during childhood. *Brain Dev* 2018;40:116-25.
 13. Cheng Q, Xu X, Zu Q, Lu S, Yu J, Liu X, Wang B, Shi H, Teng G, Liu S. High b value DWI in evaluation of the hyperacute cerebral ischemia at 3T: a comparative study in an embolic canine stroke model. *Exp Ther Med* 2016;12:951-6.
 14. Kim JH, Na DG, Chang KH, Song IC, Choi SH, Son KR, Kim KW, Sohn CH. Serial MR analysis of early permanent and transient ischemia in rats: diffusion tensor imaging and high b value diffusion weighted imaging. *Korean J Radiol* 2013;14:307-15.
 15. Miki Y, Fujioka M, Taoka T, Tanaka H, Chitoku S, Matsuyama T, Tanaka S. Utility of high-b-value diffusion-weighted magnetic resonance imaging in evaluating reversible medial longitudinal fasciculus syndrome caused by acute brainstem ischemia. *J Stroke Cerebrovasc Dis* 2015;24:e157-9.
 16. Zhu LH, Zhang ZP, Wang FN, Cheng QH, Guo G. Diffusion kurtosis imaging of microstructural changes in brain tissue affected by acute ischemic stroke in different locations. *Neural Regen Res* 2019;14:272-9.
 17. Auriat AM, Ferris JK, Peters S, Ramirez J, Black SE, Jacova C, Boyd LA. The impact of covert lacunar infarcts and white matter hyperintensities on cognitive and motor outcomes after stroke. *J Stroke Cerebrovasc Dis* 2019;28:381-8.
 18. Stys PK, Ransom BR, Waxman SG, Davis PK. Role of extracellular calcium in anoxic injury of mammalian central white matter. *Proc Natl Acad Sci U S A* 1990;87:4212-6.
 19. Dohmen C, Kumura E, Rosner G, Heiss WD, Graf R. Adenosine in relation to calcium homeostasis: comparison between gray and white matter ischemia. *J Cereb Blood Flow Metab* 2001;21:503-10.
 20. Sawada H, Udaka F, Seriu N, Shindou K, Kameyama M, Tsujimura M. MRI demonstration of cortical laminar necrosis and delayed white matter injury in anoxic encephalopathy. *Neuroradiology* 1990;32:319-21.
 21. Chen C, Bivard A, Lin L, Levi CR, Spratt NJ, Parsons MW. Thresholds for infarction vary between gray matter and white matter in acute ischemic stroke: a CT perfusion study. *J Cereb Blood Flow Metab* 2019;39:536-46.
 22. Arakawa S, Wright PM, Koga M, Phan TG, Reutens DC, Lim I, Gunawan MR, Ma H, Perera N, Ly J, Zavala J, Fitt G, Donnan GA. Ischemic thresholds for gray and white matter: a diffusion and perfusion magnetic resonance study. *Stroke* 2006;37:1211-6.
 23. Zeng Q, Shi F, Zhang J, Ling C, Dong F, Jiang B. A modified tri-exponential model for multi-b-value diffusion-weighted imaging: a method to detect the strictly diffusion-limited compartment in brain. *Front Neurosci* 2018;12:102.
 24. Mohammed NA, Abdullah DHS. Apparent diffusion coefficient value of normal brain in relation to age and gender in adults. *Ann Med Health Sci Res* 2020;10:799-803.
 25. Bai Y, Lin Y, Tian J, Shi D, Cheng J, Haacke EM, Hong X, Ma B, Zhou J, Wang M. Grading of gliomas by using monoexponential, biexponential, and stretched exponential diffusion-weighted MR imaging and diffusion kurtosis MR imaging. *Radiology* 2016;278:496-504.
 26. Helenius J, Perkiö J, Soine L, Ostergaard L, Carano RA,

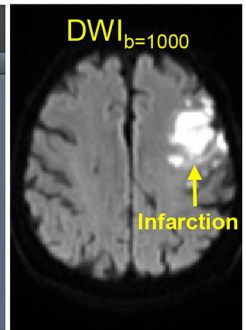
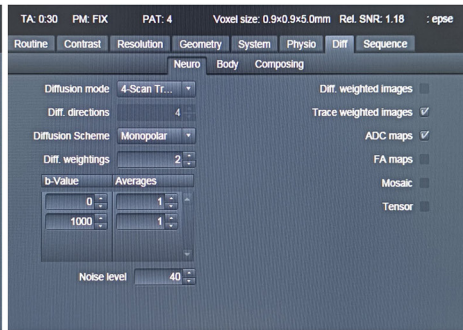
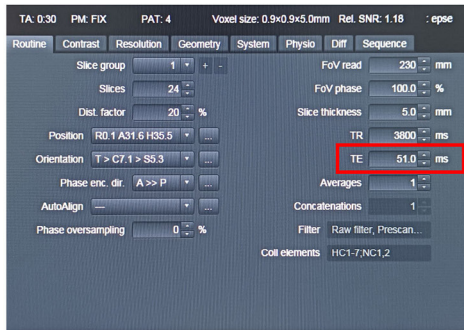
Salonen O, Savolainen S, Kaste M, Aronen HJ, Tatlisumak T. Cerebral hemodynamics in a healthy population measured by dynamic susceptibility contrast MR imaging. *Acta Radiol* 2003;44:538-46.

27. Grosser M, Gellissen S, Borchert P, Sedlacik J, Nawabi

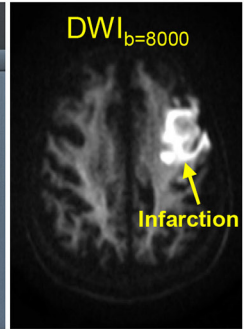
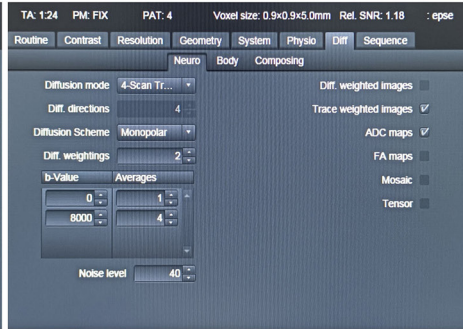
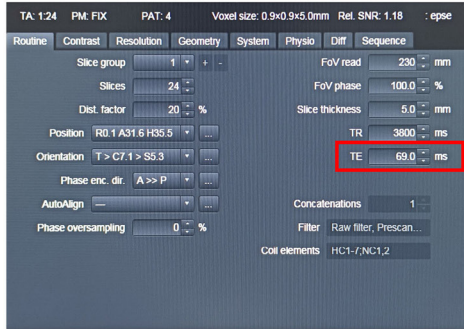
J, Fiehler J, Forkert ND. Improved multi-parametric prediction of tissue outcome in acute ischemic stroke patients using spatial features. *PLoS One* 2020;15:e0228113.

Cite this article as: Huang X, Xu X, Sun Y, Cai G, Jiang R, Chen J, Xue Y. Ultra-high b value DWI in distinguishing fresh gray matter ischemic lesions from white matter ones: a comparative study with routine and high b value DWI. *Quant Imaging Med Surg* 2021;11(11):4583-4593. doi: 10.21037/qims-20-1241

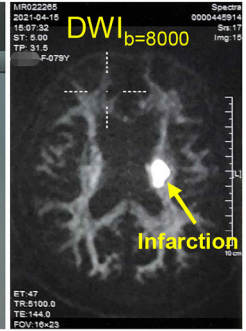
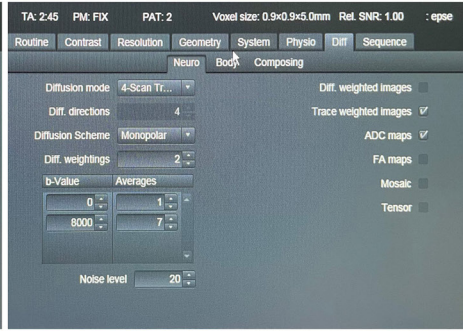
MAGNETOM
Prisma
3.0T
DWI_{b=1000}



MAGNETOM
Prisma
3.0T
DWI_{b=8000}



MAGNETOM
Spectra
3.0T
DWI_{b=8000}



MAGNETOM
Amira
1.5T
DWI_{b=6000}

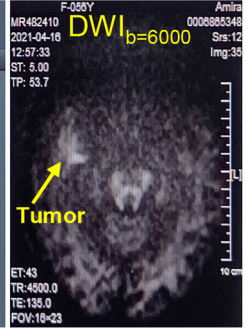
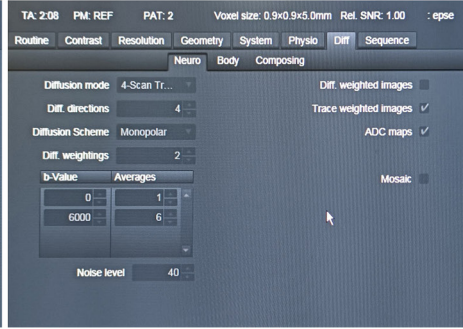
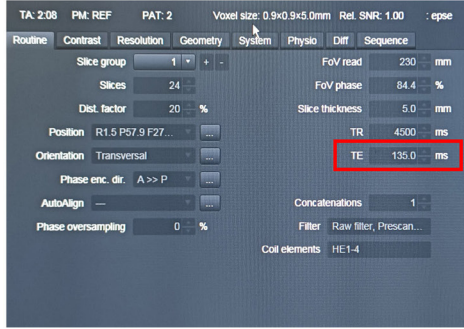


Figure S1 DWI sequence parameters on three different MR scanners. With the same voxel size, the TE were 51 ms for DWI_{b=1000} and 69 ms for DWI_{b=8000} on MAGNETOM Prisma. In contrast, the TE was 144 ms for DWI_{b=8000} on MAGNETOM Spectra and 135 ms for DWI_{b=6000} on MAGNETOM Amira, which were much longer than that on MAGNETOM Prisma. As expected, the scanner, MAGNETOM Prisma, produced the DWI images with the highest signal-to-noise ratio. Therefore, the TE is really greatly reduced on MAGNETOM Prisma. DWI, diffusion-weighted imaging; MR, magnetic resonance; TE, echo time.

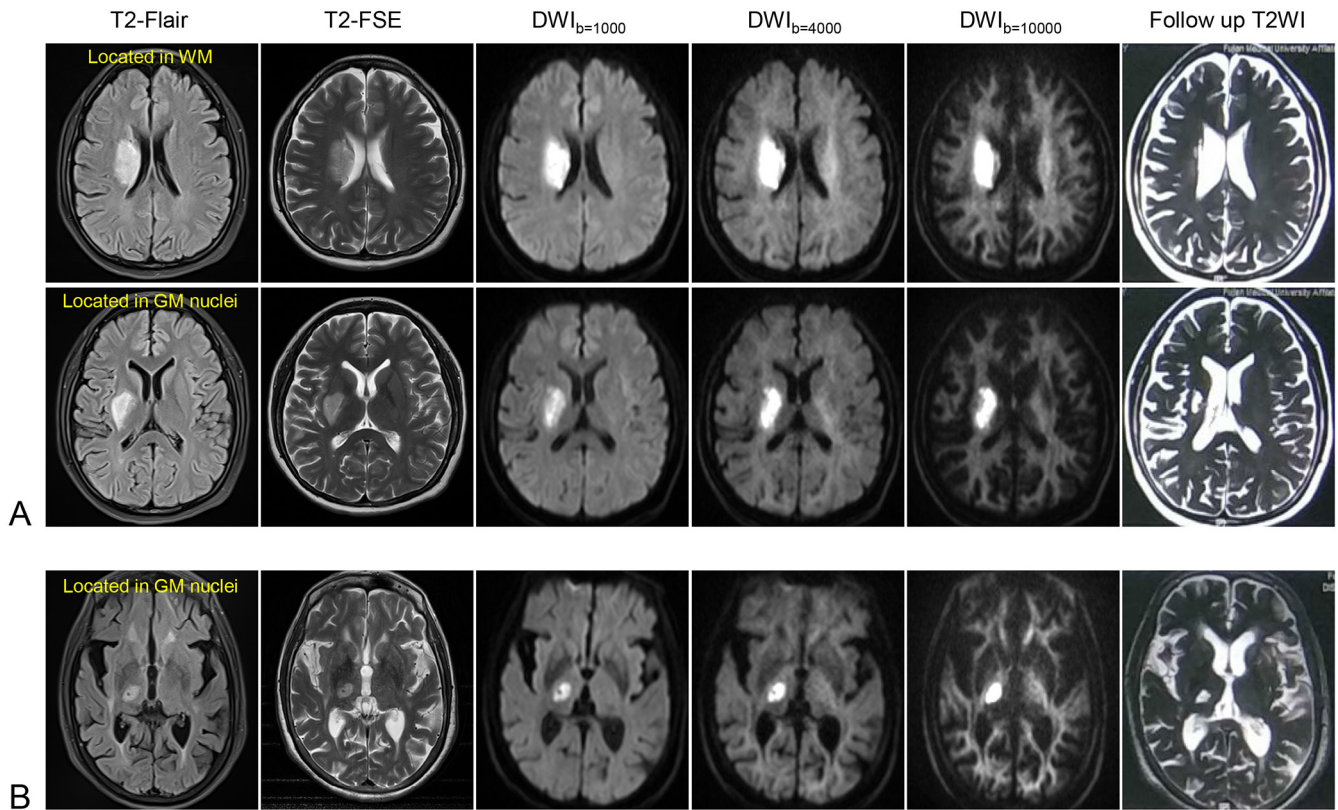


Figure S2 Two representative patients with post-treatment MRI. Patient A had two lesions located in WM and GM, respectively, whereas patient B had only one lesion located in GM. According to the MRI from these two patients, it seems that FIL in WM had a better prognosis than that in GM. MRI, magnetic resonance imaging; WM, white matter; GM, gray matter; T2-FSE, T2-fast spin echo; DWI, diffusion-weighted imaging; T2WI, T2-weighted imaging.